385

A PRACTICAL ALL-FIBER LASER VIBROMETER

by R.I. Laming, T.H. Wilmshurst, N.A. Halliwell and J.R. Baker

Since the advent of the laser, optical metrology is providing mechanical engineers with data which they previously have considered to be unobtainable. Vibration measurement in situations where the target surface is hot, light or rotating precludes the use of contacting transducers such as accelerometers and, as a result, laser vibrometers[1] have been developed to solve this problem. Their principle of operation relies on the detection of the Doppler shift in the scattered light from the target surface by heterodyne with frequency-shifted reference light from the same laser source. The frequency shift in the reference light provides a carrier frequency in the photodetector output which the Doppler shift from the target surface then frequency modulates. In this way the ambiguity in the direction of the target motion is removed.

The idea of incorporating an open air path-laser vibrometer into an all-fiber device is attractive since this would allow for remote, passive sensing of vibration in situations where direct optical access is precluded. Unfortunately, the need to frequency shift the reference light means that with commercially available frequency shifters, such as Bragg cells, the light must leave the fiber and therefore traverse a different optical path to the target light. Environmental disturbance of either target or reference optical path, in this case, is seen as spurious vibrations included in the detector output. Environmental effects such as temperature changes, acoustic pressure fluctuations or vibration of the fiber itself may change the refractive index of either light path to cause this noise. In order to provide a practical engineering instrument for on-site use these problems must be avoided. An all-fiber device will be described which was first reported in Electronics Letter.[2]

R.I. Laming is Pirelli Research Fellow, Optical Fiber Group, University of Southampton, Southampton, U.K. T.H. Wilmshurst is a Reader in Electronics, Department of Electronics and Computer Science, University of Southampton, Southampton, U.K. N.A. Halliwell is a Professor, Department of Mechanical Engineering, University of Loughborough, Loughborough, U.K. J.R. Baker is a Research Assistant, University of Southampton, Southampton, U.K.

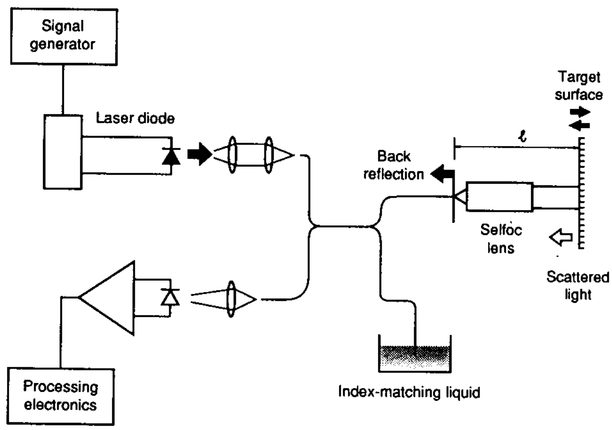

Fig. 1—*Optical geometry of the vibrometer*

PHYSICS OF OPERATION

Figure 1 shows a schematic diagram of an all-fiber laser vibrometer. With reference to this figure, frequency shifting is obtained by current modulating the laser diode to produce a small amplitude, sinusoidal variation in the output frequency. The diode light is launched into one port of a four-port single-mode fiber coupler which has one of its output ports index matched. A Selfoc lens collimates the target beam onto the surface of interest while the back reflection from the fiber end is used as the reference light. Backscattered light from the target surface re-enters the fiber and travels the same optical path as the reference light before the heterodyne occurs on the photodetector at the remaining output port of the coupler. The path length difference,[21] equivalent to twice the fiber end to target distance, causes a phase delay in the returning scattered light from the target. This produces discrete frequency components in the photodetector output at the modulation frequency and higher order harmonics. Through careful control of the current modulation of the laser diode it is possible to demodulate the photodetector output so as to produce a time-resolved voltage analog of the target surface vibration velocity.

It is important to note that the environmental noise problem described in the introduction is avoided with this geometry. Target and reference light travel identical paths through the fiber so that refractive index variations caused by a hostile environment affect both identically and are ignored in the heterodyne at the photodetector.

THEORY OF OPERATION

A sinusoidal change in the drive current to the laser diode produces a frequency shift[3] (v) in the output radiation given by

$$v = v_o + \Delta v \sin \omega_m t \tag{1}$$

where v_0 is the mean frequency, Δv is the amplitude of the shift and ω_m in the modulation frequency.

The output current of the photodetector is modulated by the cosine of the phase difference between the target signal light and the reference light reflected back from the end of the fiber at the interface with the Selfoc lens. This phase difference Φ is given by,

$$\Phi = \frac{2\pi}{c} \int_0^{2l} [v_o + \Delta v \sin \omega_m (t - \frac{x}{c})]dx \tag{2}$$

where c is the velocity of light. To a good approximation eq (2) can be written,

$$\Phi = 2kl + \frac{4\pi l \Delta v}{c} \sin(\omega_m t) \tag{3}$$

where k is the wavenumber of the light. With reference to eq (3), changes in l are dominated by the term $2kl$ which is the classical result for an interferometer of this kind. If the ratio of scattered light intensity (I_T) re-entering the fiber to the reference beam intensity (I_R) is given by α, the final result for the detector on output $i(t)$ is given by

$$i(t) = \beta I_R [1 + K \cos(\Phi_T + \Phi_m \sin \omega_m t)] \tag{4}$$

where $\beta = 1/l + \alpha, K = 2\sqrt{\alpha}/l + \alpha$
$\Phi_T = 2kl, \quad \Phi_m = 4\pi \Delta v l/c$

With reference to eq (4) the constant K is a measure of the modulation depth of the signal or 'fringe visibility' in classical terms. In practice, current modulation of the laser diode source produces amplitude as well as frequency modulation of the output so that

$$I_R = \bar{I}_R (1 + a \sin \omega_m t) \tag{5}$$

where $\bar{I}_R$ is the mean reference intensity and (a) is amplitude of the modulation. The output of the photodetector is then

$$i(t) = \beta \bar{I}_R (1 + a \sin \omega_m t)[1 + K \cos(\Phi_T + \Phi_m \sin \omega_m t)] \tag{6}$$

A signal of the form described by eq (4) can be demodulated[4] by mixing with a square wave at the fundamental frequency ω_m and maintaining the phase excursion Φ_m =2.82 rads. This is achieved through control of the frequency modulation (Δv) of the diode given by

$$\Delta v = \frac{c\Phi_m}{4\pi l} \tag{7}$$

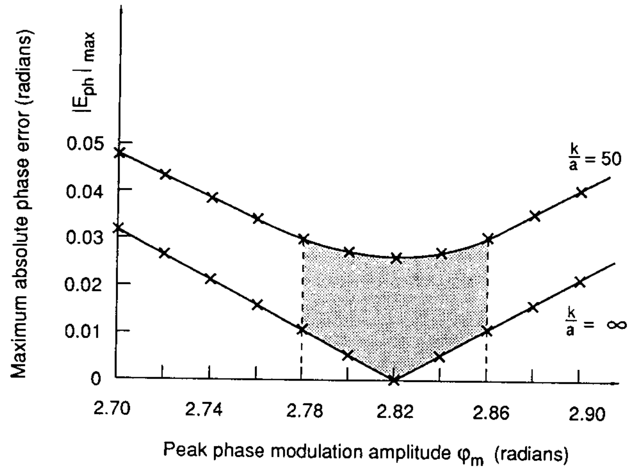

Fig. 2—*Maximum phase error*

After square wave mixing the resultant signal is bandpass filtered at a frequency $2\omega_m$ which can be expressed as

$$i(t)_{2\omega_m} = \beta \bar{I}_{ref} \cos(2\omega_m t - \Phi_T) \tag{8}$$

Frequency tracking of this signal now produces the time-resolved target surface velocity (v) according to

$$\frac{d\Phi_T}{dt} = 2k\frac{dl}{dt} = 2kv \tag{9}$$

When a signal of the form described by eq (6) is demodulated by this method the bandpass filtered signal becomes

$$i(t)_{2\omega_m} = \beta \bar{I}_{ref} \cos(2\omega_m t - \Phi_T) + \beta \bar{I}_{ref} E(t) \tag{10}$$

where

$$E(t) = (E_0 + E_1 \cos \Phi_T) \sin 2\omega_m t + E_2 \sin \Phi_T \cos 2\omega_m t \tag{11}$$

and

$$E_0 = -\frac{4a}{\pi},$$

$$E_1 = -\frac{4aK}{3\pi} J_0(\Phi_m) + \frac{Ka}{\pi} \sum_{n=1}^{\infty} (-1)^n J_{2n}(\Phi_m) \left\{\frac{1}{2n-3} - \frac{1}{2n+1} - \frac{1}{2n+3} - \frac{1}{2n-1}\right\},$$

$$E_2 = \frac{Ka}{2}\{J_1(\Phi_m) - J_3(\Phi_m)\}.$$

Given the choice of Φ_m = 2.82 rads the above 'error' terms are negligible for small (a) and the appropriate choice of the ratio (K/a). Figure 2 shows a theoretical plot of the maximum absolute phase error in (Φ_T) which can occur as a function of (Φ_m) and for different values of (K/a). For $Ka > 50$ and $\Phi_m = 2.82 \pm 0.04$ rads the maximum error is

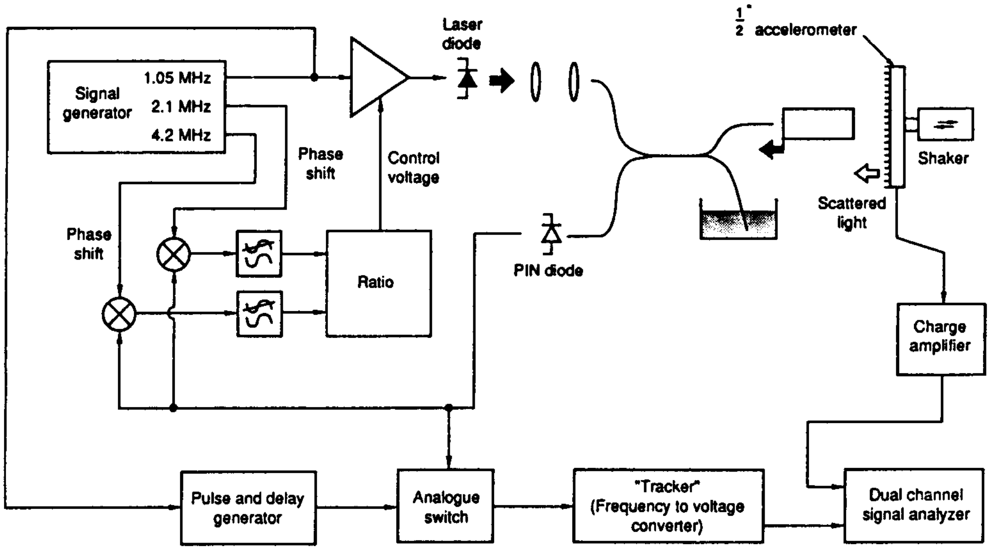

Fig. 3—*The practical system*

less than 0.03 rads which corresponds to a vibration velocity error of $0.01 f_v \mu ms^{-1}$ where f_v is the vibration frequency.

PRACTICAL SYSTEM

Figure 3 shows a schematic diagram of the practical system design. With reference to eq (4) the required value of $\Phi_m = 2.82$ rads is controlled by the frequency modulation (Δv) and the operating distance (l) of the fiber vibrometer. In order to minimize the amplitude modulation of the laser diode it is necessary to keep Δv to a minimlum and hence this dictates a minimum opeating distance for the device.

In practice, the operating distance will vary and it is therefore necessary to include an automatic feedback control for (Δv). Ignoring amplitude modulation of the laser, the detector output signal as described by eq (4) can be written.

$$i(t) = \beta \bar{I}_{ref} \{1 + K [J_0(\Phi_m) + 2 \sum_{n=1}^{\infty} J_{2n}(\Phi_m) \cos 2n\omega_m t] \cos \Phi_T - K [2 \sum_{n=0}^{\infty} j_{2n+1} \sin (2n+1)\omega_m t] \sin \Phi_T\} \qquad (12)$$

From this equation the ratio of the amplitude of the second and fourth harmonic is given by

$$J_2(\Phi_m) \cos \Phi_T : J_4(\Phi_m) \cos \Phi_T \qquad (13)$$

When $\Phi_m = 2.82$ rads this ratio takes the value 4.39 and this latter criterion is used to control the frequency modulation of the diode. It is important to note that if the mean value of Φ_T approaches $m\pi/2$; where m is an integer, the ratio defined by eq (13) would be immeasurable. However, in practice, deviations of (Φ_T) are many times π radians within the response time of the feedback loop and this control can be used successfully.

With reference to Fig. 3, the laser diode was driven at 1.05 mHz which generates sufficient frequency shift to measure vibrations up to 0.1 ms^{-1}. Signals at 2.1 and 4.2 mHz were generated and mixed with the detector output signal to generate the Bessel function ratio defined by eq (13). The latter was then used as a control voltage to an AGC amplifier to adjust the amplitude of the 1.05 mHz signal and preserve $\Phi_m = 2.82$ rads. This control then automatically compensates for laser diode temperature effects and variations in the operating distance.[1]

The detector output was synchronously gated at frequency 1.05 mHz using an analog switch and then filtered at 2.1 mHz. A frequency tracker then converted this signal to a time-resolved voltage analog of $(\dot{\Phi}_T)$, i.e., the target surface vibration velocity.

With reference to Fig. 2, the 'fringe visibility' term K is maximized when the scattered light re-entering the fiber is the same intensity as the reference light reflected from the fiber end. For a value of (a) of typically 0.02 the ratio of K/a is easily maintained at greater than 50 for an operating distance of greater than 60 mm by use of the retroreflective tape or paint on the target surface.

RESULTS AND COMPARISON WITH EXISTING TECHNIQUES

Figure 4 compares vibration velocity spectra taken with the fiber vibrometer and an accelerometer from a shaker driven at 18 kHz. The measurement bandwidth was 25.6 kHz with a resolution of 32 Hz and 100 averages were taken. With reference to this figure the vibration level at 18 kHz is in good agreement but contrary to demodulation theory[5] the fiber vibrometer noise floor does not increase with frequency. This is due to the fact that, in this case, the higher noise floor was determined by the frequency tracker used to track the $(2\omega_m)$ component.

It is important to note that, as with all laser vibrometers, it is not possible to specify a noise floor without reference to the target surface dynamic characteristics. In practice, if a target surface moves laterally or tilts, phase broadening of the Doppler signal occurs. This is manifest as spurious peaks in the vibration spectra and is a function of the laser speckle patterns dynamics on the photodetector active area. If the target surface rotates, for example, these peaks appear at the rotational speed of the target and higher order harmonics.

Figure 5 compares vibration spectra taken with the fiber vibrometer and a laser vibrometer[1] from a shaker driven at 494 Hz. The measurement bandwidth was 800 Hz with a frequency resolution of 1 Hz and 100 averages were taken. Peaks in the laser vibrometer noise floor are spurious and due to the fact that this system uses a rotating scattering surface for a reference-beam frequency shift. The fiber vibrometer noise floor is 15 dB lower and compares well with the noise floor of the accelerometer at −110 db re 1 ms^{-1} which is drawn on the figure. The measurement level at 494 Hz is in excellent agreement.

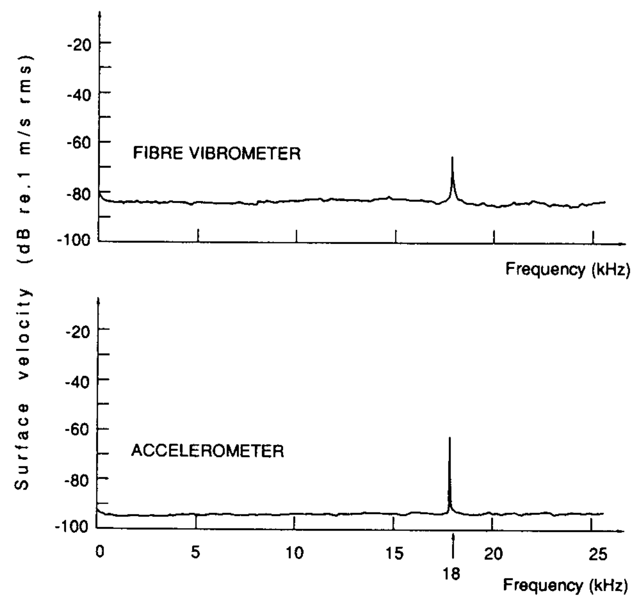

Fig. 4—*Measurement comparisons*

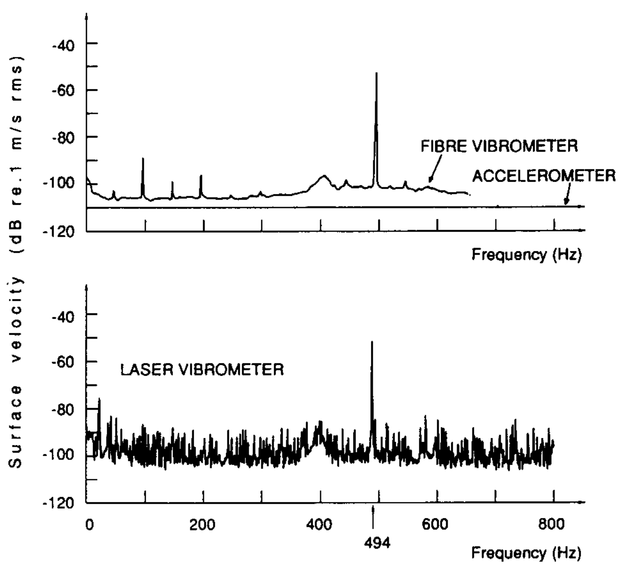

Fig. 5—*Fiber and laser vibrometer comparison*

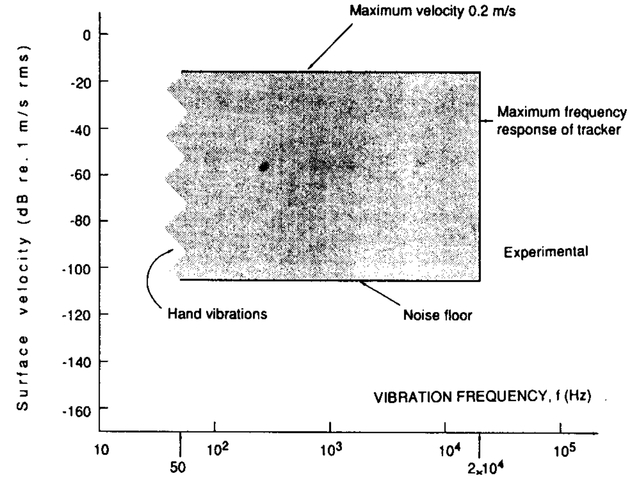

Fig. 6—*Fiber vibrometer specification*

It must be stressed that the fiber vibrometer noise floor will change if the target surface moves laterally or tilts and this is an important consideration if the device is to be hand held since the dynamics of the fiber end can produce a similar effect.

The upper velocity limit of the fiber vibrometer is determined by the sidebands of the frequencies (ω_m) and ($3\omega_m$) in the photodetector output which produce a frequency bandwidth of ±0.5 mHz equivalent to a velocity range of ±0.2 ms^{-1} in practice. The frequency response is limited at low frequencies, one to typicaly 50 Hz for hand-held use, and at high frequencies, to 20 kHz due to the frequency tracker. For normal to surface movement of the target surface, Fig. 6 collates the results for the noise floor, dynamic range and frequency response. The maximum operating distance from the target surface was designed as 300 mm but this can be extended through circuit modifications.

CONCLUSIONS

A design of a practical all-fiber laser vibrometer has been demonstrated which compares well in performance to existing techniques but offers the extra advantages of passive, remote sensing of vibration. The fiber vibrometer is well suited to hand-held use since it has the potential for robust, lightweight construction and is insensitive to environmental disturbances.

REFERENCES

1. *Pickering, C.J.D., Halliwell,, N.A. and Wilmshurst, T.H., "The Laser Vibrometer: A Portable Instrument," Journal of Sound and Vibration,* **107** *(3), 471-485 (1986).*
2. *Laming, R.I., Gold, M.P., Payne, D.N. and Halliwell, N.A., "Fibre optic vibration probe," Electronic Letters,* **22** *(3), 167-168 (1986).*
3. *Dandridge, A. and Goldberg, I., "Current-induced frequency modulation in diode lasers," Electron. Lett.,* **18**, *302-304 (1982).*
4. *Kim, B.Y. and Shaw, H.T., "Phase-reading all fibre-optic gyroscope," Optics Letters,* **9**, *378-380 (1984).*
5. *Betts, J.A., "Signal processing, modulation and noise," Unibooks: Hodder and Stoughton, 106-118.*